

Supplementary Information for Electronic structure of quasi-one-dimensional superconductor $K_2Cr_3As_3$ from first-principles calculations

by Hao Jiang, Guanghan Cao and Chao Cao

Relativistic DOS and PDOS of $K_2Cr_3As_3$ with experimental structure

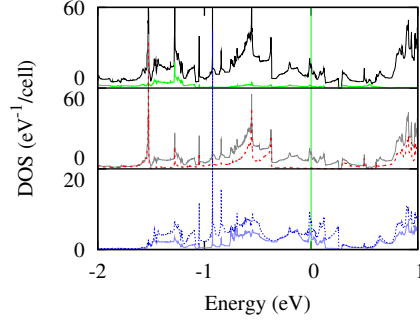


FIG. S-1: Total and projected DOS from relativistic calculations. The upper panel shows the total DOS (black line) and PDOS from As-4p (green line); middle and bottom panel shows the PDOS from all five-orbitals of Cr-3d (grey lines in the middle panel), the PDOS of Cr-3d_{xx} and Cr-3d_{yy} (red line in the middle panel), and the PDOS of Cr-3d_{zz} (light blue line in the bottom panel), Cr-3d_{x²-y²} and Cr-3d_{xy} (blue line in the bottom panel).

We show here in FIG. S-1a the DOS and PDOS of $K_2Cr_3As_3$ from relativistic calculations (with SOC effect included). The lattice constants and internal coordinates from experiment were employed. The orbital contribution close to E_F remains the same as non-relativistic calculations.

Electronic structure with fully optimized structure

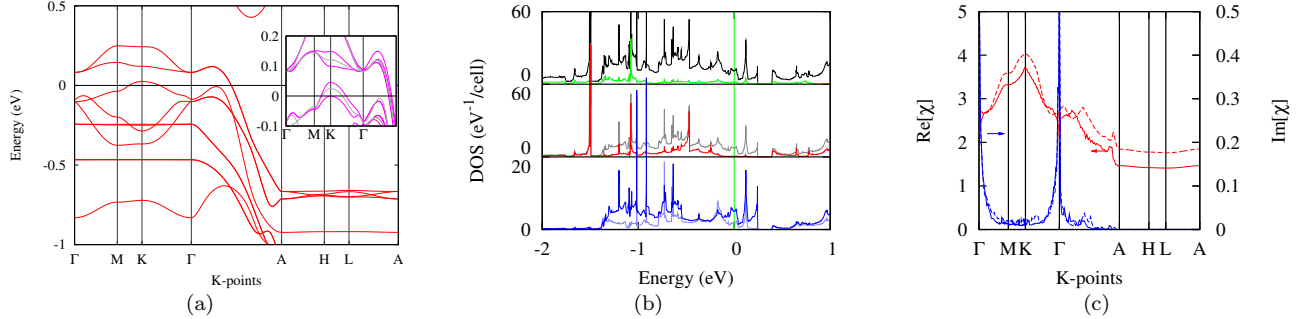


FIG. S-2: (a) Relativistic and non-relativistic band structure, (b) non-relativistic DOS and (c) bare electron susceptibility of $K_2Cr_3As_3$ with optimized lattice constants and internal coordinates. In panel a), the red lines show the non-relativistic result (without SOC effect) and the blue lines show the relativistic result (with SOC effect). In (b), upper panel shows the total DOS (black line) and PDOS from As-4p (green line); middle and bottom panel shows the PDOS from all five-orbitals of Cr-3d (grey lines in the middle panel), the PDOS of Cr-3d_{xx} and Cr-3d_{yy} (red line in the middle panel), and the PDOS of Cr-3d_{zz} (light blue line in the bottom panel), Cr-3d_{x²-y²} and Cr-3d_{xy} (blue line in the bottom panel). In (c), The red and blue lines are the real and imaginary part of χ , respectively. The solid and dashed lines are results for pristine $K_2Cr_3As_3$ and 0.2 hole doped $K_2Cr_3As_3$, respectively.

We show here the band structure (FIG. S-2a) and DOS (FIG. S-2b) of $K_2Cr_3As_3$ with optimized lattice constants and internal coordinates. The most profound change in the band structure is that the γ band is submerged below E_F

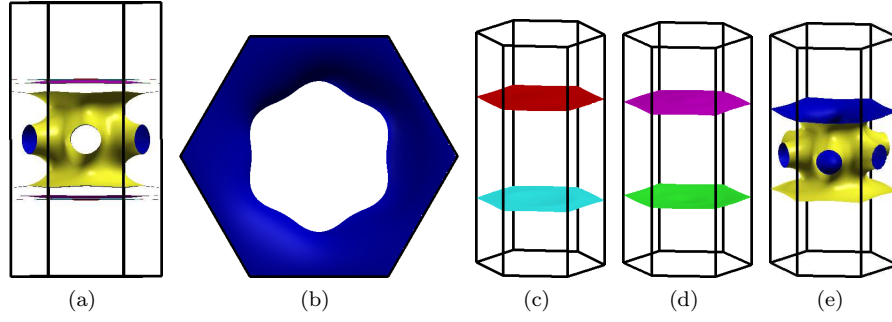


FIG. S-3: Non-relativistic Fermi surface sheets of $\text{K}_2\text{Cr}_3\text{As}_3$ with optimized lattice constants and internal coordinates. (a) Side-view of all sheets superposed. (b) Top view of 3D γ band sheet. (c-e) 3D view of α , β , and γ band sheets, respectively. The choice of high symmetry points is the same as FIG. 3c.

around Γ after structural relaxation. This will lead to a topologically different Fermi surface sheet (FIG. S-3(b-c)) from the one shown in FIG. 3(e-f). The α and β bands are less affected (FIG. S-3(c-d)). The number of bands crossing E_F , and their respective orbital character remains the same. Also, it is apparent that the SOC effect is large on γ and β , but is almost negligible for α (inset of FIG. S-2a).

The resulting non-relativistic band structure was also fitted to a 10-orbital tight-binding Hamiltonian using MLWF. Using this Hamiltonian, we have also calculated the bare electron susceptibility of both pristine $\text{K}_2\text{Cr}_3\text{As}_3$ and 0.2 hole doped $\text{K}_2\text{Cr}_3\text{As}_3$ (or, $\text{K}_{1.8}\text{Cr}_3\text{As}_3$) (FIG. S-2c). Despite of the detailed changes in the band structure, the prominent peak of $\text{Im}\chi_0$ at Γ is insensitive to the structural change.

Electronic structure with idealized structure

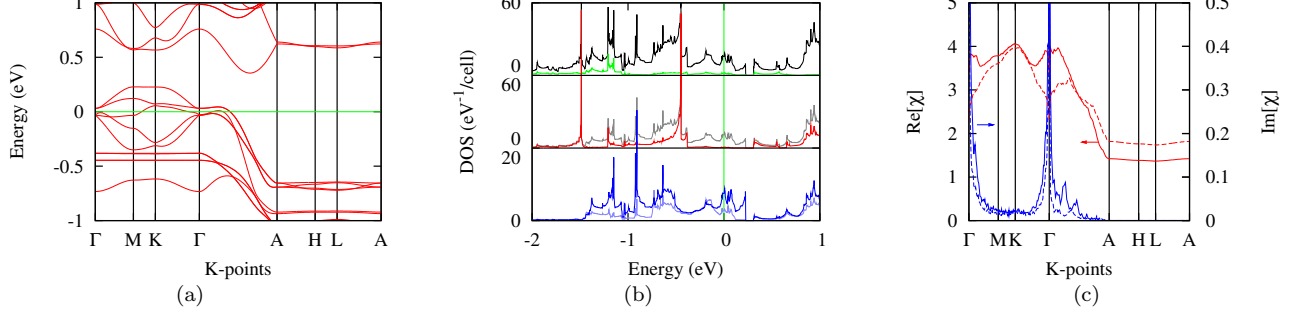


FIG. S-4: Non-relativistic (a) band structure (b) DOS and (c) bare electron susceptibility of $\text{K}_2\text{Cr}_3\text{As}_3$ with idealized structure. In panel (b), upper panel shows the total DOS (black line) and PDOS from As-4p (green line); middle and bottom panel shows the PDOS from all five-orbitals of Cr-3d (grey lines in the middle panel), the PDOS of Cr-3d_{zx} and Cr-3d_{zy} (red line in the middle panel), and the PDOS of Cr-3d_{z²} (light blue line in the bottom panel), Cr-3d_{x²-y²} and Cr-3d_{xy} (blue line in the bottom panel). In panel (c), the red and blue lines are the real and imaginary part of χ , respectively. The solid and dashed lines are results for pristine $\text{K}_2\text{Cr}_3\text{As}_3$ and 0.2 hole doped $\text{K}_2\text{Cr}_3\text{As}_3$, respectively.

We have also calculated the nonrelativistic electronic structure of $\text{K}_2\text{Cr}_3\text{As}_3$ with an idealized structure, i.e. the Cr_6 cluster forms an ideal octahedron without distortion. We show here the band structure (FIG. S-4a), DOS (FIG. S-4b), bare electron susceptibility χ_0 (FIG. S-4c) and Fermi surface sheets (FIG. S-5). As indicated in these results, the number of bands crossing E_F , the respective orbital characters and dimensionality characters of these bands, the number of Fermi surface sheets and the prominent peak of $\text{Im}\chi_0$ at Γ are insensitive to the structural change.

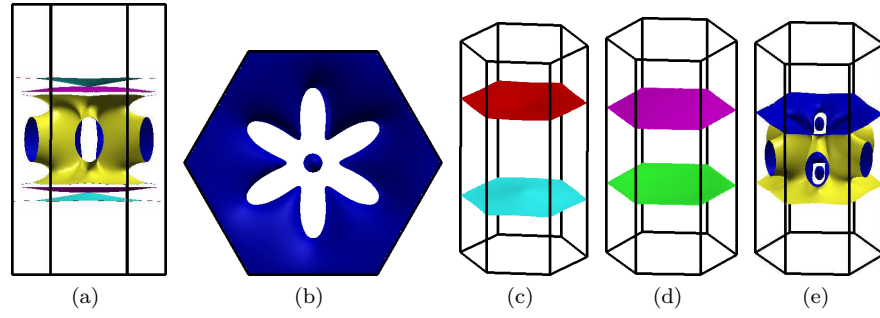


FIG. S-5: Non-relativistic Fermi surface sheets of $\text{K}_2\text{Cr}_3\text{As}_3$ with an idealized structure. (a) Side-view of all sheets superposed. (b) Top view of 3D γ band sheet. (c-e) 3D view of α , β , and γ band sheets, respectively. The choice of high symmetry points is the same as FIG. 3c.

Electronic structure at DFT+ U level

Figure S-6 shows the electronic structure of $\text{K}_2\text{Cr}_3\text{As}_3$ under DFT+ U with $U=2.0$ eV and $J=0.7$ eV. The band structure, DOS, Fermi surfaces and bare electron susceptibility are almost identical to those without U , suggesting that DFT+ U is not very effective in the current system and will not affect our main conclusions.

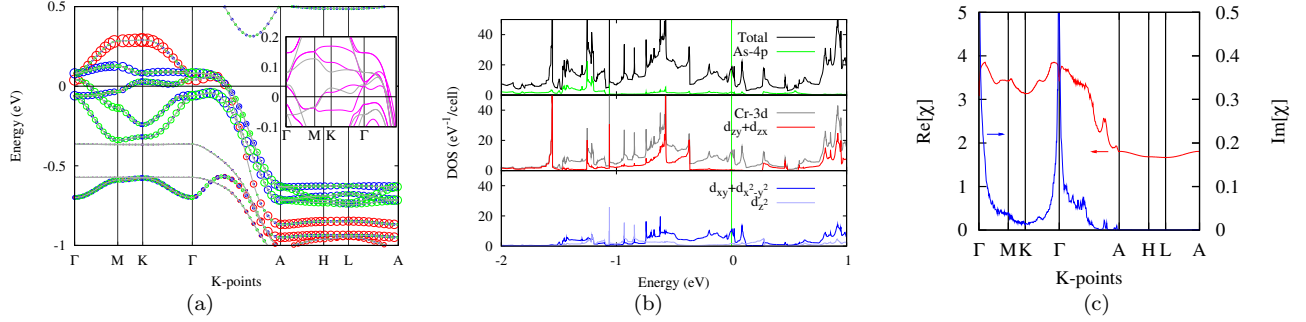


FIG. S-6: (a) Electronic band structure (b) Electron density of states and (c) Bare electron susceptibility of $\text{K}_2\text{Cr}_3\text{As}_3$ with experimental structure at $U=2.0$ eV and $J=0.7$ eV. In panel (a), the inset shows comparison between relativistic (magenta solid lines) and non-relativistic (grey solid lines) results. The size of the red, blue and green circles are proportional to the contributions from the d_{z^2} , $d_{x^2-y^2}$ and d_{xy} orbitals, respectively. In (b), the upper panel shows the total DOS (black line) and PDOS from As-4p (green line); middle and bottom panel shows the PDOS from all five-orbitals of Cr-3d (grey lines in the middle panel), the PDOS of Cr-3d $_{zx}$ and Cr-3d $_{zy}$ (red line in the middle panel), and the PDOS of Cr-3d $_{z^2}$ (light blue line in the bottom panel), Cr-3d $_{x^2-y^2}$ and Cr-3d $_{xy}$ (blue line in the bottom panel).